communications physics

Article

https://doi.org/10.1038/s42005-025-01949-x

Carrier-envelope-phase characterization of ultrafast mid-infrared laser pulses through harmonic generation and interference in argon

Claudia Gollner[1,3], Valentina Shumakova[1,4], Jacob Barker[2], Audrius Pugžlys[1], Andrius Baltuška[1] & Pavel Polynkin[2]

The propagation of an intense, femtosecond, mid-infrared laser pulse in a gaseous medium results in the efficient generation of spectrally overlapping low-order harmonics, whose optical carrier phases are linked to the carrier-envelope phase (CEP) of the mid-infrared driver pulse. Random peak-power fluctuations of the driver pulses, converted to the fluctuations of the nonlinear phases, acquired by the pulses on propagation, cause this phase correlation to smear out. We show that this seemingly irreversible loss of phase can be recovered, and that the complete information needed for the phase correction is contained in the harmonic spectra itself. The optical phases of the intense driver pulse and its harmonics, as fragile as they appear to be against even weak disturbances, evolve deterministically during highly nonlinear propagation through the extended ionization region.

Dramatic progress in laser technology in the past three decades has resulted in a paradigm shift in ultrafast science from cycle-averaged (or envelope) physics to studies of sub-cycle (or field-resolved) strong-field processes[1,2]. The CEP of the laser pulse became an important parameter determining the outcome of strong-field interactions driven by intense, few-cycle laser pulses[3]. This development has enabled numerous exciting applications including molecular fingerprinting of complex biological molecules in their natural environment with high sensitivity and specificity[4]. In situations involving the propagation of intense laser pulses through media in the presence of ionization, the CEP coherence is fragile, and precise control over the energy and duration of the laser pulses is needed for its preservation, as even small fluctuations of the peak power of the pulses result in smearing out the phase information due to the amplitude-to-phase coupling. Intuitively, the more intense the laser pulses are, and the longer the nonlinear interaction region is, the more vulnerable the absolute optical phase is to the fluctuations of the peak power of the pulses. It has been argued that nonlinear self-channeling of intense laser pulses in transparent media, commonly referred to as filamentation[5,6], results in a complete and irreversible loss of phase information[7].

Nonlinear propagation of intense laser pulses in gaseous media has been extensively studied using near-infrared (NIR) femtosecond laser sources based on Ti:Sapphire gain medium. The preservation of the CEP coherence on the passage of the laser pulse through the extended interaction region has been demonstrated, but it imposed stringent requirements on the stability of the laser source, with less than 1% pulse-to-pulse energy fluctuations[8]. The ongoing developments of the ultrafast laser technology enable investigations in strong-field science, including the studies of the laser self-action effects in gaseous media in new, long-wavelength regimes—short-wave, mid-wave, and long-wave infrared (SWIR, MIR, and LWIR, respectively)[9–11].

Two key features of the interactions of intense, SWIR and MIR laser fields with gases have become evident: The efficient, non-perturbative generation of low-order, odd-harmonics of the driver pulse[12,13] and the importance of absorption resonances due to trace constituents of the gas, e.g., water vapor and carbon dioxide in the case of propagation in air[14,15]. The two major mechanisms of low-order harmonic generation in gases are the perturbative nonlinear $\chi^{(3)}$ response of the bound electrons in gas molecules and molecular ions and the Brunel mechanism, which relies on the stepwise, sub-cycle ionization buildup and the associated effective current[16]. With NIR drivers, the $\chi^{(3)}$ mechanism dominates, and the energy of the generated low-order harmonics drops significantly from one harmonic order to the next. In MIR, on the contrary, the low-order harmonic generation is dominated by the Brunel mechanism, and the energies of several lowest-order harmonics can be comparable[17].

[1]Photonics Institute, Vienna University of Technology, Vienna, Austria. [2]College of Optical Sciences, The University of Arizona, Tucson, AZ, USA. [3]Present address: SLAC National Accelerator Laboratory, Menlo Park, CA, USA. [4]Present address: UltraFast Innovations Gmbh, Dieselstr. 5, Garching (Munich), 85748, Germany. e-mail: ppolynkin@optics.arizona.edu

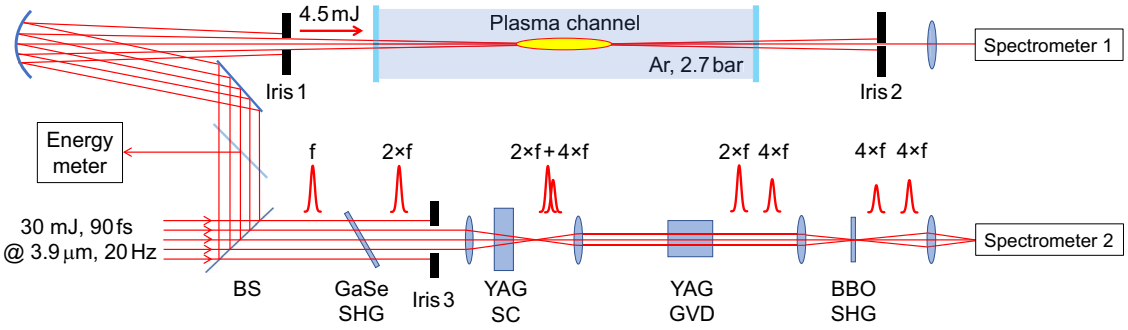

Fig. 1 | Experimental setup. BS: 55%:45% (T:R) pellicle beam splitter, SHG: second harmonic generator, SC: supercontinuum generator (8 mm-thick YAG plate), GVD: group-velocity dispersion generator (10 mm-long YAG rod), BBO: Beta barium borate. The propagation of the MIR pulse and its harmonics through the *f*–2*f* interferometer arm of the setup is illustrated by the corresponding waveforms above the beam path in the lower part of the figure.

The harmonics generated by both the Brunel and the $\chi^{(3)}$ mechanisms are of odd orders, and for each individual pulse, they are phase-coherent with the MIR driver pulse. In the dispersionless and weakly nonlinear case, in which the driver pulse propagates nearly undisturbed, the generated harmonics have optical phases equal to the CEP of the driver pulse times the harmonic order. This is not the situation we consider. As the intense MIR pulse propagates through the nonlinear interaction zone, its spatiotemporal waveform experiences complex evolution driven by various linear and nonlinear interactions. Although the generated harmonics remain coherent with the MIR driver for each individual pulse, this phase relationship is complex, and intuitively, it is expected to be unrecoverable in the presence of the shot-to-shot peak power fluctuations of the MIR pulses. Our results will show that this intuition is incorrect.

In a recent study of filamentation of few-cycle laser pulses at 1.7 μm wavelength in air, it has been shown that the CEP of the SWIR driver pulse is rigidly linked to the phase of the spectral interference between the overlapping spectral tails of the supercontinuum and the third harmonic of the driver, generated on propagation through the interaction zone[18]. The laser source used in that work was CEP-stable and operated at a 1 kHz pulse repetition rate. The demonstrated relation between the CEP of the laser pulses and the phase of the spectral interference between the supercontinuum and the third-order harmonic of the driver has been averaged over multiple laser shots and survived the averaging. Here, we show that spectral interference of this sort can be used for the CEP characterization of intense MIR laser pulses on a shot-by-shot basis, but in this case, the interference is between the neighboring odd-order harmonics of the driver pulse. We experimentally correlate the phase of the spectral interference between neighboring harmonics, generated in argon gas, with the CEP of the input MIR pulse, measured (to an undefined additive constant), in parallel, by *f*–2*f* interferometry of its second harmonic. The phase information, seemingly lost on the highly nonlinear propagation through the extended interaction region, is shown to be recoverable using a post-correction based on the spectral data itself. Harmonic interference of the sort we discuss here has been observed in transparent solid-state media, both passive[19,20] and active[21], as well as in high-harmonic emission in argon gas[22].

The importance of our results is twofold: It has been suggested that under certain conditions, the on-axis component of the pulse propagating nonlinearly in the presence of ionization self-compresses to few optical cycles[23]. The knowledge of the CEP of the generated few-cycle optical transient may add to the practical utility of this self-compression effect for applications. Furthermore, our results suggest that strong-field experiments that require CEP stability can be conducted with CEP-unstable lasers with the aid of the data sorting according to the CEP values of the driver pulses, deduced on a shot-by-shot basis from the spectral interference measurements. Our results add to the wide range of methods developed for the CEP characterization of ultrashort laser pulses, ranging from the early work[24] to the recently reported sophisticated approaches including the technique for spatial CEP mapping of complex spatio-temporal light waveforms[25].

Methods

Experimental setup

Our experimental setup is schematically shown in Fig. 1. The 3.9 μm optical parametric chirped-pulse amplification (OPCPA) source is capable of generating up to 30 mJ of energy per pulse, with 90 fs pulse duration, at 20 pulses per second[26]. The source is not CEP-stable, and the CEP of the pulses fluctuates randomly from one laser shot to the next. Relatively large shot-to-shot pulse-energy fluctuations with the RMS standard deviation of about 0.9 mJ (the standard deviation over a mean of about 3%), as well as significant, but not precisely characterized, fluctuations of the pulse duration are expected to scramble the optical phase information on the highly nonlinear propagation of the laser pulses through the ionized gas, as a result of the above-mentioned nonlinear amplitude-to-phase coupling.

The MIR laser beam is split into two beams. The first beam, shown in the top part of Fig. 1, passes through a 4.5 mm-diameter aperture (Iris 1 in Fig. 1) and, after the aperture, on average, has 4.5 mJ of energy per pulse. It is focused with an $f = 50$ cm concave mirror, at a nearly normal angle of incidence, into a cell filled with argon at 2.7 bar of pressure. Based on the $\propto\lambda^2$ scaling of the critical power for self-focusing with the wavelength of the source and its inverse scaling with the gas pressure, the 50 GW peak power of the MIR pulses entering the gas cell is about 60% of the critical power for self-focusing[27,28]. Since the peak power of the driver pulses is below the self-focusing threshold, we can estimate the field parameters in the interaction zone using the formulas for linear beam focusing, which yield the values of 300 μm and 40 mm for the focused beam diameter and twice its Rayleigh range, respectively. The latter value is consistent with the length of the plasma channel, whose fluorescence is observed through the transparent wall of the gas cell. The peak optical intensity in the interaction volume, also estimated linearly, is about 80 TW/cm^2. The peak plasma density at that intensity level and 90 fs pulse duration are estimated at 7×10^{16} cm^{-3}[29], which, somewhat coincidentally, is of the same order as the density of electrons in NIR air filaments[30].

The spectrum of the white light generated on the nonlinear propagation through the interaction zone contains multiple odd-order harmonics of the MIR driver. The spectral regions where the neighboring harmonics overlap exhibit interference, whose phase we will attempt to correlate with the CEP of the MIR driver pulses. The harmonic emission consists of the on-axis and conical parts. In the on-axis part, different spectral components of the emission propagate collinearly. In the conical part, they propagate at different angles of up to about 0.6° with respect to the beam axis. As we discuss below, spectral interference is due to the emissions into the neighboring harmonics at different locations along the interaction region. Accordingly, clear spectral interference between the neighboring harmonics is observed only in the on-axis component of the emission, where emissions into the neighboring harmonics are spatially overlapping. This on-axis emission component is selected by an aperture (Iris 2 in Fig. 1), before being focused on the entrance slit of a VIS–NIR spectrometer. The selection of propagation medium (argon gas), gas pressure, focusing conditions for the

MIR beam entering the gas cell, and pulse energy have been all adjusted to optimize the generation of low-order harmonics and their spectral overlap.

Note that we have observed harmonic spectral interference, discussed here for the case of propagation in argon, also in ambient air using MIR pulses with the peak power above the self-focusing threshold. In air, the effect was not as apparent as in argon under the optimum conditions. Experiments in air focused on the analysis of the angularly-resolved harmonic emissions. Their results will be presented in a separate publication.

The second beam, shown in the lower part of Fig. 1, is used to quantify the CEP of the incoming MIR pulses, to an arbitrary additive constant and on a shot-by-shot basis, using inline *f*–2*f* interferometry[24]. Since this technique involves the measurement of an optical spectrum, and high-resolution single-shot spectrometers are readily available only for the UV–VIS–NIR spectral range, it is technically much simpler to apply the *f*–2*f* CEP characterization to the second harmonic of the MIR pulses rather than to the MIR pulses themselves. Accordingly, the MIR signal is frequency doubled in a 100 μm-thick GaSe crystal and directed to the interferometer, which, in this case, measures the CEP of the second harmonic of the MIR pulses (i.e., 2 × CEP of the MIR pulses themselves). The components of the interferometer are specified in the caption for Fig. 1. In order to optimize supercontinuum generation in the 8 mm-thick yttrium aluminum garnet (YAG) plate, the energy of the second harmonic pulse, generated in the 100 μm-thick GaSe crystal, was attenuated by angle-detuning the crystal from the orientation for maximum conversion, and the beam was passed through the 3 mm-diameter aperture. The pulse energy in the second harmonic after the aperture was about 7.5 μJ on average, fluctuating by about 3% RMS. This pulse energy is sufficiently low to ensure linear propagation through the lenses and the dispersive YAG rod in the *f*−2*f* interferometer.

The dominant contribution to the uncertainty in the measurement of the CEP phase by the *f*−2*f* interferometer is from the nonlinear propagation of the second harmonic pulse through the supercontinuum-generating YAG plate. This type of error has been studied in detail in ref. 24. Following that analysis, we estimate that the uncertainty of the CEP measurement by the *f*−2*f* interferometer in our setup, associated with the shot-to-shot fluctuations of the peak power of the pulses, is of the order of one radian. This error alone is sufficiently large to smear out the correlation between the optical phases that our experiment is aiming to establish. The data sorting procedure discussed below is essential for removing this phase uncertainty, as well as the uncertainty of the phase of the harmonic spectral interference measured in the argon arm of the experimental setup, both uncertainties being due to the peak-power fluctuations of the MIR laser pulses.

The energy of the incoming MIR pulses was also measured for every laser shot by a calibrated energy meter and recorded into a file. The entire experimental setup was assembled on a rigid (not floating) optical table and not covered, subjecting it to the vibrations and airflow typical for an optics laboratory environment. The goal of our experiment is to establish a correlation between the phase of the spectral interference between the neighboring harmonics and 2 × CEP of the MIR driver, independently measured by the *f*−2*f* interferometer, thereby showing that the CEP coherence is preserved on the nonlinear propagation of the MIR laser pulses through the ~4 cm— long ionization region.

A typical spectrum of the VIS-NIR portion of the on-axis emission in the upper arm of the setup is shown in Fig. 2a. The shaded area in the plot covers the region of the fifth harmonic of the MIR pulse, which is attenuated by multiple color-glass filters with a non-trivial dependence of attenuation on wavelength. The filters are used to prevent the spectrometer from being saturated by the strong fifth-harmonic signal while having an acceptable level of signal in the spectral regions of interest, where the neighboring harmonics overlap and interfere. The meaningful parts of the spectrum are to the left and to the right from the shaded area, where interferences between the fifth and seventh harmonics and the third and fifth harmonics, respectively, are evident. Note that it has been suggested that including in the analysis the shaded area, where all three harmonics interfere, may yield additional information about the CEP of the MIR laser pulses in the interaction region[31]. The validation of such a proposition is beyond the scope of the present study.

To determine the phases of the harmonic spectral interference, we select two spectral intervals covering one oscillation period each, in the regions of overlaps of the fifth and seventh harmonics, as well as of the third and fifth harmonics, as indicated by the dashed vertical lines in Fig. 2a. The wavelengths corresponding to the interference maxima, which we determine from the spectra numerically, are linearly mapped onto the phases of the spectral interference within the phase interval $[-\pi, \pi]$.

In Fig. 2b, we show examples of spectra in the spectral region of overlap of the third and fifth harmonics generated in argon for two different, randomly selected laser shots. The corresponding spectra recorded in the *f*−2*f* arm of the setup are shown in Fig. 2c. As in the case of harmonic

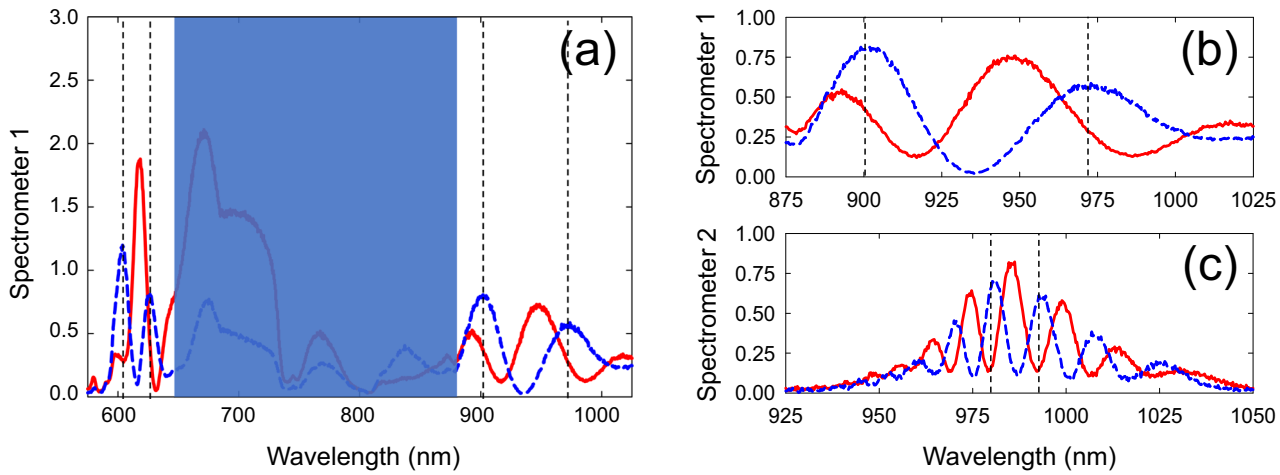

Fig. 2 | Examples of spectrometer data. a VIS–NIR spectra of the on-axis emission, generated in argon, for two randomly selected laser shots, shown with red and blue lines. The shaded area covers the spectral region attenuated by multiple color-glass filters with not precisely characterized dependence of transmission on wavelength, to prevent the spectrometer from saturation by strong fifth-harmonic emission. This spectral interval is unimportant for the present analysis. The regions to the left and to the right from the shaded area contain interfering spectral tails of the fifth and seventh harmonics and the third and fifth harmonics of the MIR driver, respectively. **b** A closeup of the spectral region to the right from the shaded area in **a**, containing spectral interference between the third and fifth harmonics, for two randomly selected laser shots, shown with red and blue lines. **c** Spectra recorded by the *f*−2*f* interferometer arm of the experimental setup for the same laser shots as those used in (**a**) and (**b**). In all three panels, the dashed vertical lines encompass one complete oscillation period, selected to determine the values of the interference phases.

interference, the 2 × CEP phase, measured by the $f-2f$ interferometer, is determined by linearly mapping the location of the spectral peak within a pre-selected spectral interval, corresponding to one complete oscillation period, onto the phase interval $[-\pi, \pi]$.

In total, spectra generated by about 12,000 laser shots were recorded in parallel in the two arms of the setup. Because of the technical restrictions imposed by the data collection system, the spectra were recorded at four shots per second, by triggering the two spectrometers on every fifth laser shot. The entire duration of data collection was about fifty minutes. In addition to the spectral data, the values of the pulse energy for every laser shot were also measured and recorded. About 10% of all recorded shots turned out to be low-energy outliers. The harmonic spectra produced by them contained no meaningful interference signal, and those shots have been discarded.

Quantifying phase correlation

The correlation between the phases of interference between different harmonics, as well as the correlation between those phases and 2 × CEP of the MIR driver, measured by the $f-2f$ interferometer, are evaluated visually from the correlation plots and quantified by computing the standard deviation between the two phases to be correlated:

$$\sigma^{(1,2)} = \sqrt{(1/N)\,\Sigma_{i=1}^{N}\left[\left(\phi_i^{(1)} - \phi_i^{(2)} - \Delta\right)_{\mathrm{mod}\,\pi}\right]^2} \qquad (1)$$

Here, $\phi_i^{(1)}$ and $\phi_i^{(2)}$ are the values of the two phases to be correlated for i^{th} laser shot, with both phases defined on the interval $[-\pi; \pi]$. Δ is the constant overall offset between the two phases for the data sets in which the correlation between the two phases is evident. For the data sets where no correlation between the two phases is present, the value of Δ can be set to zero. The summation is over all N recorded spectra with random values of the CEP of the MIR driver pulses. For the data set with perfectly correlated phases, $\sigma^{(1,2)} = 0$, while for the data set with completely uncorrelated phases, $\sigma^{(1,2)} = [\int_{-\pi}^{\pi} x^2 \mathrm{d}x/2\pi]^{1/2} = \sqrt{1/3}\,\pi \approx 1.81$ rad.

Data processing

The goal of our experiment is to search for the correlation between the phase of the spectral interference of the neighboring harmonics generated in argon and the 2 × CEP phase independently measured by the $f-2f$ interferometer. As evident from the data, shown below, the correlation appears to be smeared out due to the shot-to-shot fluctuations of the peak power of the pulses and the associated amplitude-to-phase coupling. To recover the correlation, we use the following data processing procedure. For each laser shot, we compute S, the integral of the VIS-NIR part of the spectrum, generated in argon, over the entire detection range of Spectrometer 1—from 550 nm to 1.1 μm. This integral, measured in arbitrary units and normalized to 1, is the metric of the peak power of the incident MIR pulse, and its value reflects the fluctuations of both the input pulse energy and its duration. (While the measurement of the former is straightforward, the single-shot characterization of the latter is far from it.) As shown in Fig. 3a, b, the correlation between the phase of interference between the third and fifth harmonics and 2 × CEP, measured by the $f-2f$ interferometer, is clearly present for the subsets of the laser shots selected to have S, the values of the integrated VIS–NIR spectrum, within a narrow range (about 5% of the total range of variation of the integrated spectrum over all laser shots for the data shown).

The correlation plots for the subsets of laser shots, selected according to the integrated VIS–NIR spectrum within different narrow ranges, have phase offsets Δ, relative to zero phase, that vary depending on the value of the spectral integral S, as shown in Fig. 3c (see also Fig. S2b–d in Supplementary

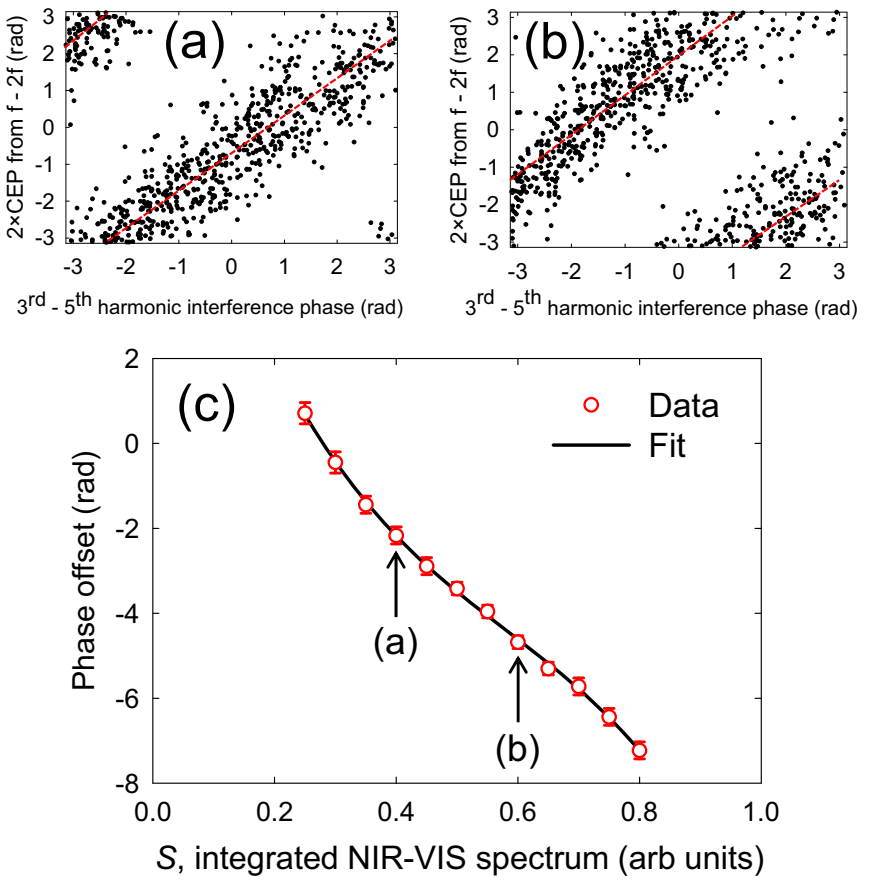

Fig. 3 | Data processing procedure. a, **b** Subsets of the correlation data for two particular narrow intervals of the spectral density integrated from 550 nm to 1.1 μm: (0.400 ± 0.025) arb. units (**a**) and (0.600 ± 0.025) arb. units (**b**). The normalized integrated spectral density varies from ~0.15 to 1.0 arb. units over all recorded laser shots without the low-energy outliers that accounted for about 10% of all shots and have been discarded. **c** The phase offset vs. the integrated spectral density, inferred from the subsets of the correlation data with the integrated spectral density being within 5% of the maximum value of that integral over all shots. The data points shown with red circles are the results of linear fitting of the subsets of the correlation data. The error bars are based on the uncertainty of the linear fitting. The black solid line is a third-order polynomial fit to the data points, specified in Eq. (2). The two vertical arrows point to the two specific values of the integrated spectrum, corresponding to the two correlation plots shown in (**a**) and ((**b**).

Methods: Data processing procedure. There, Δ is shown as "Phase offset" for three different sub-sets of laser shots, selected by having the associated values of integrated NIR–VIS spectrum within 5% of the three particular values, specified in the plots). The dependence $\Delta(S)$, inferred from the data, is continuous, deterministic, and close to linear. For the particular experimental realization discussed here, it is well represented by a third-order polynomial fit explicitly given by

$$\Delta_{\mathrm{fit}}(S) = 9.75 - 51.06 \cdot S + 68.90 \cdot S^2 - 39.50 \cdot S^3 \quad (2)$$

(Note that the fitted phase offset Δ_{fit} is a continuous function of S, not restricted to the interval $[-\pi; \pi]$, thus facilitating the fitting by a continuous third-order polynomial function.) For every recorded laser shot, we compute S, the value of the integrated VIS–NIR spectrum, and subtract the phase offset, quantified by the fit formula (2) with that value of S, from ϕ_{3-5}, the measured phase of the spectral interference between the third and fifth harmonics for that shot:

$$\phi_{3-5}^{(\mathrm{corrected})} = \phi_{3-5} - \Delta_{\mathrm{fit}}(S) \quad (3)$$

The data processing procedure we use is further explained in Supplementary Methods: Data processing procedure.

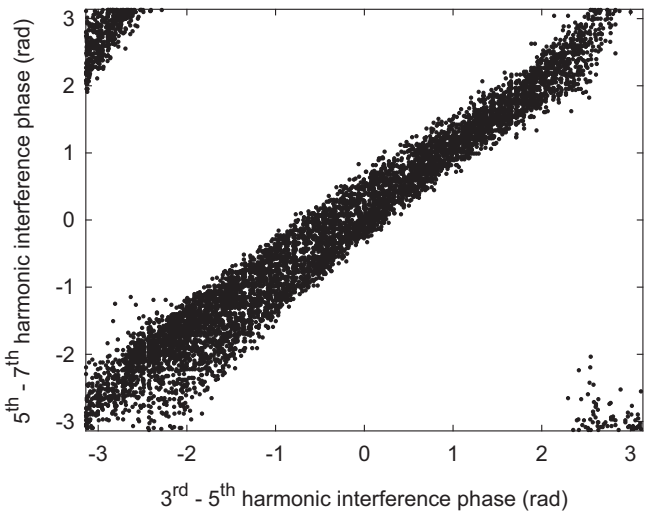

Fig. 4 | Correlation between phases of spectral interference of two different pairs of neighboring harmonics. The phase of the spectral interference between the fifth and seventh harmonics vs. the phase of the spectral interference between the third and fifth harmonics. No data post-processing was applied, except for discarding the low-energy outlier shots that generated no overlapping harmonic spectra (about 10% of all shots).

Results

The phases of the spectral interference between the third and fifth harmonics and between the fifth and seventh harmonics are visually well correlated, as evident in the correlation plot shown in Fig. 4. The corresponding value of $\sigma^{(1,2)}$, defined in Eq. (1), is 0.36 rad. No data post-processing has been applied, and the two phases are well correlated in spite of the significant shot-to-shot fluctuations of the MIR pulse energy and duration.

In Fig. 5a, we show a plot of the phase of the spectral interference between the third and fifth harmonics vs. the value of 2 × CEP measured in the $f-2f$ arm of the setup. The correlation between the two phases is seemingly absent. The nonlinear beam self-action effects could suppress the phase noise resulting from the amplitude-to-phase coupling, as analyzed, e.g., in ref. 32. However, as evident from our results, the random shot-to-shot fluctuations of the peak power of the pulses are large enough to completely smear out the phase correlation between the input MIR driver pulses and the phases of the low-order harmonics generated on propagation through the interaction region. The value of the standard deviation for the data shown in Fig. 5a is $\sigma^{(1,2)} = 1.86$ rad, which is the same as the theoretical value for completely uncorrelated data, within the accuracy of determining the interference phases.

The apparent loss of phase coherence is recovered using the spectral data itself using the data post-processing procedure discussed above in the Methods: Data processing section. The resulting corrected correlation plot is shown in Fig. 5b. The correlation between the corrected phases of the harmonic spectral interference and the values of 2 × CEP, independently measured in the $f-2f$ arm of the setup, is clearly restored, with the corresponding value of the standard deviation $\sigma^{(1,2)} = 1.06$ rad. This proves that over several meters of propagation through the open-air experimental setup, including highly nonlinear propagation through the ionization region, and over the entire duration of the data collection (~50 min), the phase relationship between the incident MIR pulse and the generated harmonics varied predictably with the peak power of the driver pulses, quantified through the total integrated VIS–NIR spectrum.

As we found, our data processing procedure worked best when using the integrated NIR–VIS spectrum of the on-axis harmonics generated in

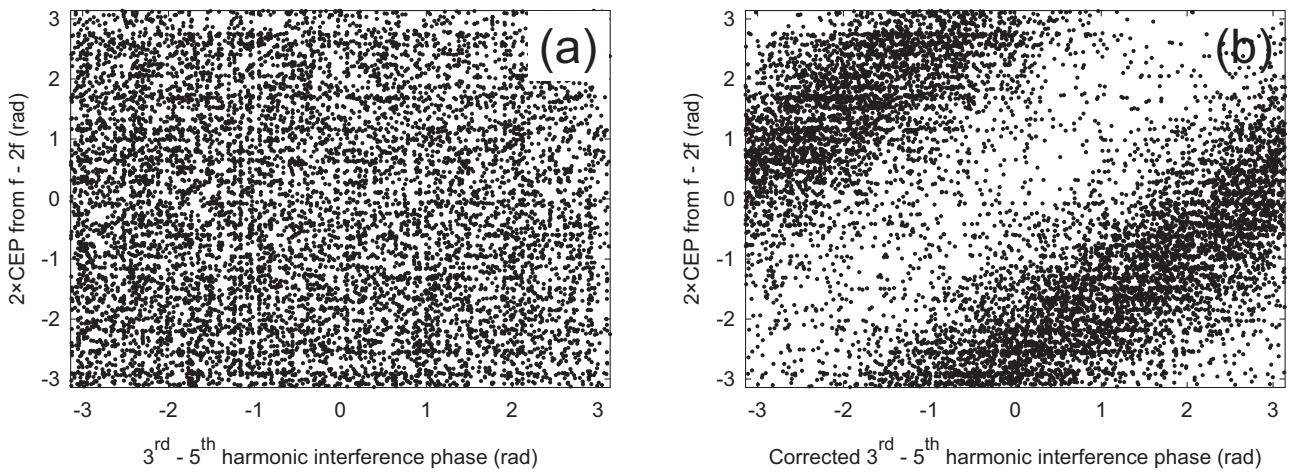

Fig. 5 | Phase correlation plots before and after the application of the data post-processing procedure. a 2 × CEP of the laser pulses measured by the $f-2f$ interferometer vs. the phase of the spectral interference between the third and fifth harmonics, before data post-processing. The correlation is smeared out due to the shot-to-shot fluctuations of the peak power of the MIR driver pulses. **b** The correlation plot after the application of the data post-processing procedure. After correction, the two phases are correlated with the value of the standard deviation, defined in Eq. (1), of 1.06 rad.

argon, for quantifying the peak-power-dependent offset between the two phases to be correlated. We also have applied the same procedure using the the integrated spectrum in the $f-2f$ arm of the setup and the values of the pulse energy, for quantifying the phase offset. The procedure worked in both cases, although not as well as when the integrated NIR–VIS spectrum of harmonics was used. Data correction based on the integrated spectrum in the $f-2f$ arm still resulted in a clearly discernible correlation with the value of the standard deviation $\sigma^{(1,2)} = 1.42$, whereas the correlation in the data corrected using the values of the pulse energy was barely noticeable. In that latter case, the corresponding value of the standard deviation $\sigma^{(1,2)} = 1.62$, which is close to the theoretical value for completely uncorrelated phase values. (For details, see Supplementary Results: Data processing using different parametrizations of the peak-power-dependent phase offset.) Based on the data, we conclude that the contributions of the shot-to-shot pulse energy and pulse duration fluctuations to the fluctuations of the peak power of the MIR pulses are comparable.

Discussion

The mechanism behind harmonic spectral interference discussed here is as follows: As the intense MIR driver pulse propagates through the ionization region, it continuously generates odd-order harmonics. At the same time, the spectrum of the driver is broadened by the combined action of self-phase modulation and plasma blue shifting. On the rising edge of the pulse, the two spectral broadening mechanisms act in opposition, while on the trailing edge, they enhance each other. As a result, the spectrum of the pulse primarily extends to the blue side. At a certain position near the end of the interaction region, a particular odd-order harmonic, generated at that point by the blue-shifted driver pulse, starts spectrally overlapping with the neighboring higher-order harmonic, generated earlier. The period of the spectral interference for a particular pair of neighboring harmonics is determined by the temporal delay by which the group-velocity dispersion of the generated plasma retards the mid-infrared driver pulse relative to the generated higher-order harmonic in the harmonic pair, over the length of the ionization region. The spectral interference periods derived from the data are 70 nm for the interference between the third and fifth harmonics and 25 nm for the interference between the fifth and seventh harmonics. These values correspond to the delays of about 40 and 50 fs, respectively, both delays being comparable to the duration of the MIR driver pulse.

What is required for the data post-processing procedure discussed above to be effective in the recovery of the CEP of the MIR driver pulses is that the blue shift of the MIR pulses is large enough for the spectra of the neighboring low-order harmonics generated on propagation to overlap. Also, the group delay between the harmonics and the MIR driver pulse in the plasma should be sufficiently large for the spectral interference to contain at least one observable interference period. The question of how restrictive these conditions are remains open and will be the subject of a future investigation.

Conclusions

We have experimentally demonstrated that the phase of the spectral interference between the neighboring odd-order harmonics, generated on the nonlinear propagation of a MIR laser pulse in argon gas, is correlated with the CEP of the MIR driver pulse. The value of the integrated harmonic spectrum is an adequate metric of the shot-to-shot fluctuations of the peak power of the incoming MIR pulses; it contains complete information about the resulting quasi-random phase shifts accumulated on the nonlinear propagation through the ionization region, and no additional experimental data is needed to quantify those fluctuations. With a proper calibration based on the values of the integrated harmonic spectrum, harmonic spectral interference can be used for the single-shot characterization of the CEPs of intense, MIR laser pulses. This characterization method enables strong-field experiments that require CEP stability to be performed with CEP-unstable sources, through the post-selection of the experimental data based on the CEP values inferred from the spectral interference measurements.

Data availability

The experimental data discussed here can be made available upon reasonable request.

Received: 13 June 2024; Accepted: 10 January 2025;
Published online: 21 January 2025

References

1. Brabec, T. & Krausz, F. Intense few-cycle laser fields: frontiers of nonlinear optics. *Rev. Mod. Phys.* **72**, 545 (2000).
2. Krausz, F. & Ivanov, M. Attosecond physics. *Rev. Mod. Phys.* **81**, 163 (2009).
3. Baltuška, A. et al. Attosecond control of electronic processes by intense light fields. *Nature* **421**, 611 (2003).
4. Pupeza, I. et al. Field-resolved infrared spectroscopy of biological systems. *Nature* **577**, 52 (2020).
5. Couairon, A. & Mysytowicz, A. Femtosecond filamentation in transparent media. *Phys. Rep.* **441**, 47 (2007).
6. Berge, L., Skupin, S., Nuter, R., Kasparian, J. & Wolf, J.-P. Ultrashort filaments of light in weakly-ionized, optically-transparent media. *Rep. Prog. Phys.* **70**, 1633 (2007).
7. Shim, B., Schrauth, S. E., Gaeta, A. L., Klein, M. & Fibich, G. Loss of phase of collapsing beams. *Phys. Rev. Lett.* **108**, 043902 (2012).
8. Guandalini, A. et al. 5.1 fs pulses generated by filamentation and carrier envelope phase stability analysis. *J. Phys. B* **39**, S257 (2006).
9. Kartashov, D. et al. Mid-infrared laser filamentation in molecular gases. *Opt. Lett.* **38**, 3194 (2013).
10. Mitrofanov, A. V. et al. Mid-infrared laser filaments in the atmosphere. *Sci. Rep.* **5**, 8368 (2015).
11. Tochitsky, S. et al. Megafilament in air formed by self-guided terawatt long-wavelength infrared laser. *Nat. Photonics* **13**, 41 (2019).
12. Kartashov, D. et al. White light generation over three octaves by femtosecond filament at 3.9 μm in argon. *Opt. Lett.* **37**, 3456 (2012).
13. Jang, D. et al. Efficient terahertz and Brunel harmonic generation from air plasma via mid-infrared coherent control. *Optica* **6**, 1338 (2019).
14. Shumakova, V. et al. Filamentation of mid-IR pulses in ambient air in the vicinity of molecular resonances. *Opt. Lett.* **43**, 2185 (2018).
15. Panov, N. A. et al. Supercontinuum of a 3.9 μm filament in air: formation of a two-octave plateau and nonlinearly enhanced linear absorption. *Phys. Rev. A* **94**, 041801 (2016).
16. Brunel, F. Harmonic generation due to plasma effects in a gas undergoing multiphoton ionization in the high-intensity limit. *J. Opt. Soc. Am. B* **7**, 521 (1990).
17. Serebryannikov, E. E. & Zheltikov, A. M. Quantum and semiclassical physics behind ultrafast optical nonlinearity in the midinfrared: the role of ionization dynamics within the field half cycle. *Phys. Rev. Lett.* **113**, 043901 (2014).
18. Ren, X. et al. In-line spectral interferometry in shortwave-infrared laser filaments in air. *Phys. Rev. Lett.* **123**, 223203 (2019).
19. Darginavičius, J. et al. Ultrabroadband supercontinuum and third-harmonic generation in bulk solids with two optical-cycle carrier-envelope phase-stable pulses at 2 μm. *Opt. Express* **21**, 25210 (2013).
20. Hollinger, R. et al. Carrier-envelope-phase measurement of few-cycle mid-infrared laser pulses using high harmonic generation in ZnO. *Opt. Express* **28**, 7314 (2020).
21. Vasilyev, S. et al. Octave-spanning Cr:ZnS femtosecond laser with intrinsic nonlinear interferometry. *Optica* **6**, 126 (2019).
22. Sansone, G. et al. Measurement of harmonic phase difference by interference of attosecond light pulses. *Phys. Rev. Lett.* **94**, 193903 (2005).
23. Bergé, L., Rolle, J. & Köhler, C. Enhanced self-compression of mid-infrared laser filaments in argon. *Phys. Rev. A* **88**, 023816 (2013).
24. Baltuška, A. et al. Phase-controlled amplification of few-cycle laser pulses. *IEEE J. Sel. Top. Quant. Electr.* **9**, 972 (2003).

25. Hanus, V. et al. Carrier-envelope phase on-chip scanner and control of laser beams. *Nat. Commun* **14**, 5068 (2023).
26. Andriukaitis, G. et al. 90 GW peak power mid-infrared pulses from an optical parametric amplifier. *Opt. Lett.* **36**, 2755 (2011).
27. Lehmeier, H. J., Leupacher, W. & Penzkofer, A. Nonresonant third order hyperpolarizability of rare gases and N_2 determined by third harmonic generation. *Opt. Commun* **56**, 67 (1985).
28. Zahedpour, S., Wahlstrand, J. K. & Milchberg, H. M. Measurement of the nonlinear refractive index of air constituents at mid-infrared wavelengths. *Opt. Lett.* **40**, 5794 (2015).
29. Bergé, L., Rolle, J. & Köhler, C. Enhanced self-compression of mid-infrared laser filaments in argon. *Phys. Rev. B* **88**, 023816 (2013).
30. Chen, Y.-H., Varma, S., Antonsen, T. M. & Milchberg, H. M. Direct measurement of the electron density of extended femtosecond laser pulse-induced filaments. *Phys. Rev. Lett.* **105**, 215005 (2010).
31. Kartashov, D., Balčiūnas, T., Andriukaitis, G., Pugžlys, A. & Baltuška, A. Absolute and relative determination of CEP from the interference of multiple low-order harmonics. CLEO Europe/EQEC, Munich, Germany, 2011, paper EG3_4.
32. Brahms, C. & Travers, J. C. Timing and energy stability of resonant dispersive wave emission in gas-filled hollow-core waveguides. *J. Phys. Photonics* **3**, 025004 (2021).

Acknowledgements

This material is based upon work supported by the U.S. Air Force Office of Scientific Research under MURI award No. FA9550-16-1-0013, by the U.S. Office of Naval Research under the award No. N00014-21-1-2469, and by the U.S. Joint Directed Energy Transition Office (JDETO). V.S. acknowledges the support from grant no. T-1216 by the Austrian Science Fund. J.B. acknowledges the support from the SMART scholarship by the US Air Force Research Laboratory and the graduate fellowship by the Directed Energy Professional Society. P.P. thanks Miroslav Kolesik, for the fruitful discussions.

Author contributions

A.P., A.B., and P.P. conceptualized and planned the study, C.G., V.S., and P.P. conducted the experiment, V.S., J.B., and P.P. analyzed the data, P.P. prepared the manuscript.

Competing interests

The authors declare no competing interests.

Additional information

Supplementary information The online version contains supplementary material available at https://doi.org/10.1038/s42005-025-01949-x.

Correspondence and requests for materials should be addressed to Pavel Polynkin.

Peer review information *Communications Physics* thanks the anonymous reviewers for their contribution to the peer review of this work.